

Supporting information for

Tuning the electronic structure of PtRu bimetallic nanoparticles for promoting hydrogen oxidation reaction in alkaline media

Chang Long^{a,b,c,†}, Kun Wang^{c,†}, Yanan Shi^c, Zhongjie Yang^c, Xiaofei Zhang^{a,b,c}, Yin Zhang^c, Jianyu Han^c, Yini Bao^d, Lin Chang^c, Shaoqin Liu^{a,b*}, and Zhiyong Tang^{c*}

^a School of Materials Science and Engineering, Harbin Institute of Technology, Harbin 150080, P. R. China.

^b MOE Key Laboratory of Micro-systems and Micro-structures Manufacturing, Harbin Institute of Technology, Harbin 150080, P. R. China.

^c CAS Key Laboratory of Nanosystem and Hierarchical Fabrication CAS Center for Excellence in Nanoscience, National Center for Nanoscience and Technology, Beijing 100190, P. R. China.

^d West China Hospital of Stomatology, Sichuan University, Chengdu 610041, PR China

Corresponding address:

zytang@nanoctr.cn

shaoqinliu@hit.edu.cn

Supplementary Content

Figure S1. Polarization curves in Ar-saturated 0.1 M KOH.

Figure S2. Electrochemical behavior of Pt-H_{ad} interaction.

Figure S3. Electrochemical surface area measurements.

Figure S4. Tafel plots of PtRu bimetallic nanoparticles and Pt/C

Figure S5. Micro-kinetic polarization plots.

Figure S6. Polarization curves and Koutecky–Levich plots.

Figure S7. ECSA-normalized kinetic current densities.

Figure S8. HOR activity comparison.

Table S1. Summary of ICP-MS results for PtRu bimetallic nanoparticles.

Table S2. Summary of binding energies for Pt 4f_{7/2} and Pt 4f_{5/2} of PtRu bimetallic nanoparticles and Pt/C from XPS results

Table S3. Summary of electrochemical surface areas for PtRu bimetallic nanoparticles and Pt/C.

Table S4. Normalized exchange current densities for PtRu bimetallic nanoparticles and Pt/C.

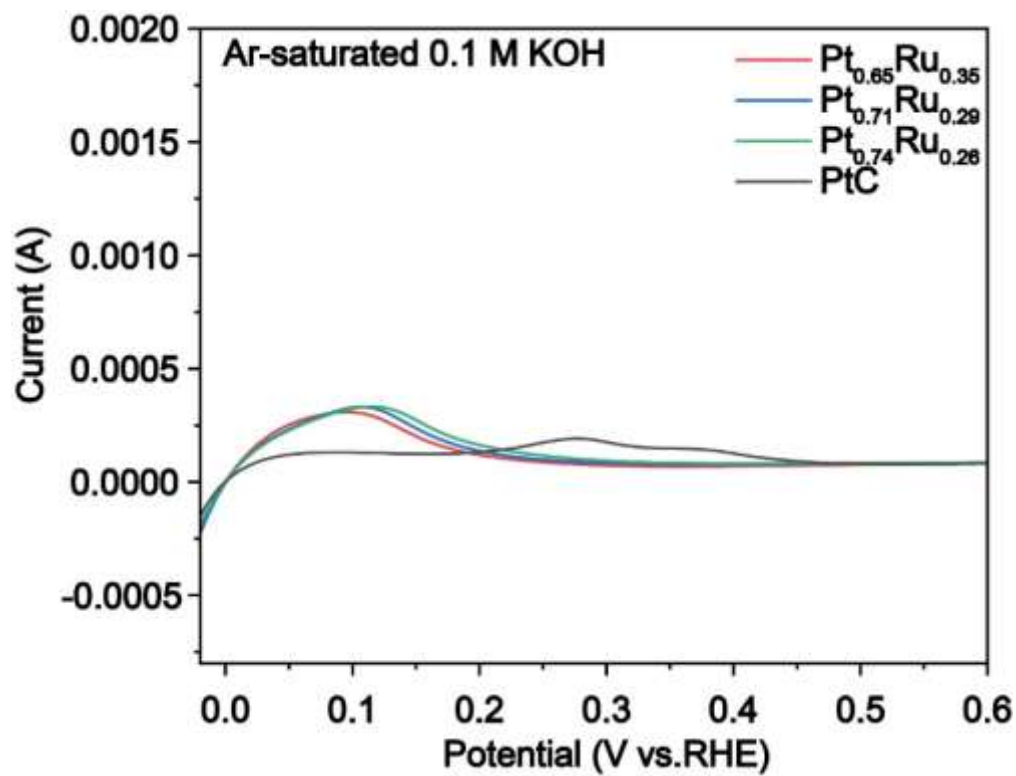


Figure S1. Polarization curves of PtRu bimetallic nanoparticles, and Pt/C in Ar-saturated 0.1 M KOH at a scan rate of 5 mV s⁻¹ under rotating speed of 1600 r.p.m.

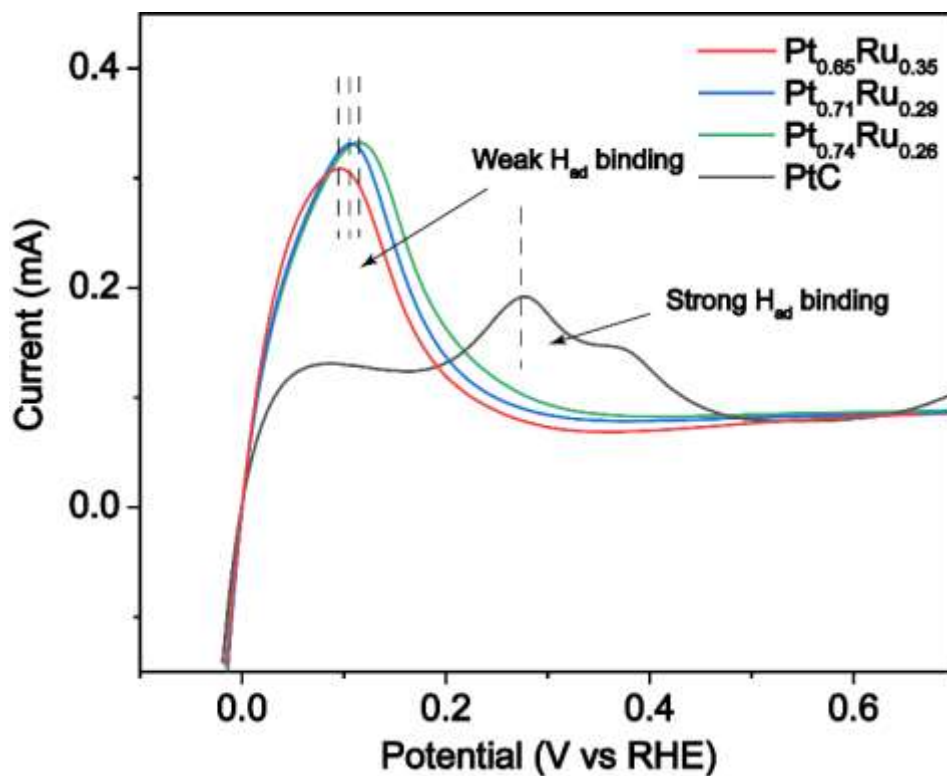


Figure S2. The impact of alloy degree on the Pt- H_{ad} interaction determined by electrochemical behavior of as-prepared catalysts in degassed 0.1 M KOH solution.

As displayed in **Figure S2**, the negative shift of oxidation peak of H_{ad} has been observed and this result indicates that the hydrogen-binding strength can be weakened according to the increased alloy degree.

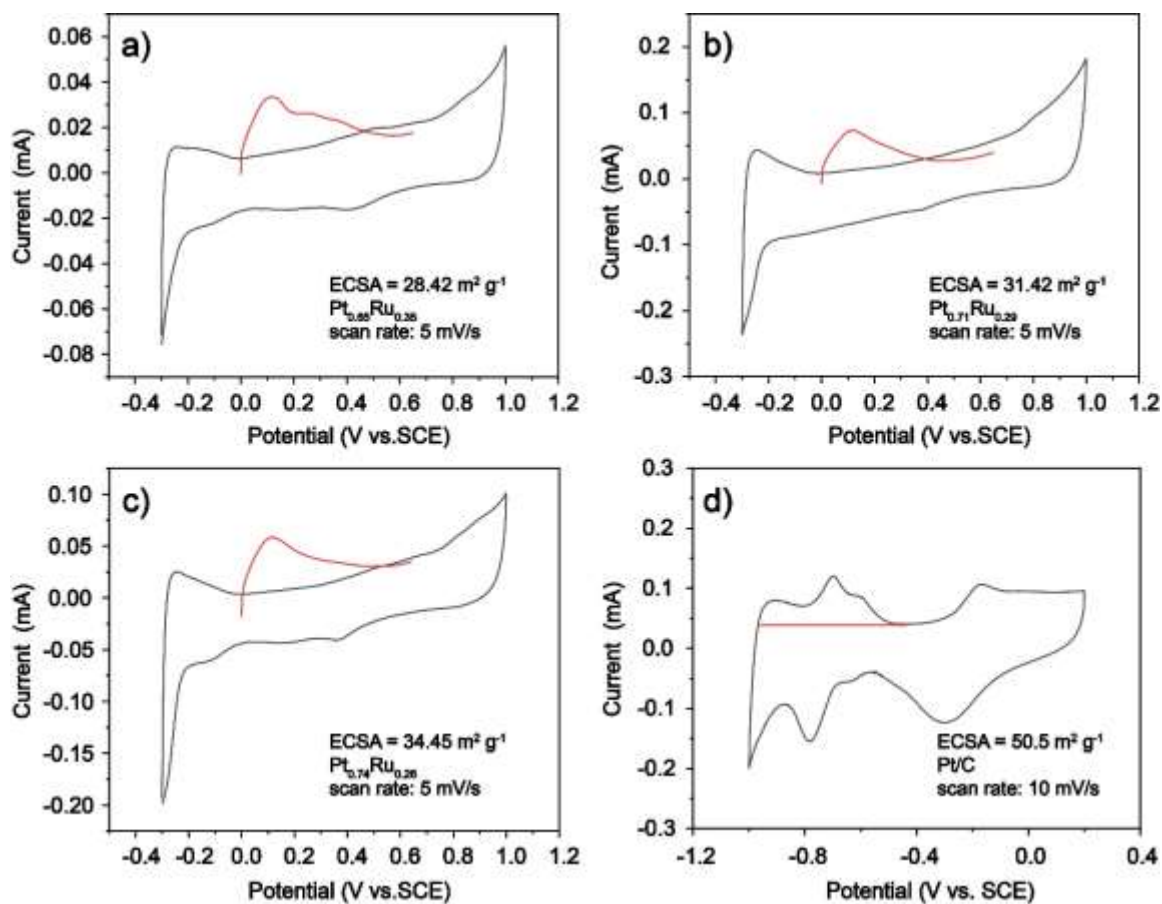


Figure S3. Electrochemical surface area measurements. a-c) Cu stripping on PtRu bimetallic nanoparticles for determining the specific surface area of Pt. d) H adsorption on Pt/C for determining the specific surface area of Pt.

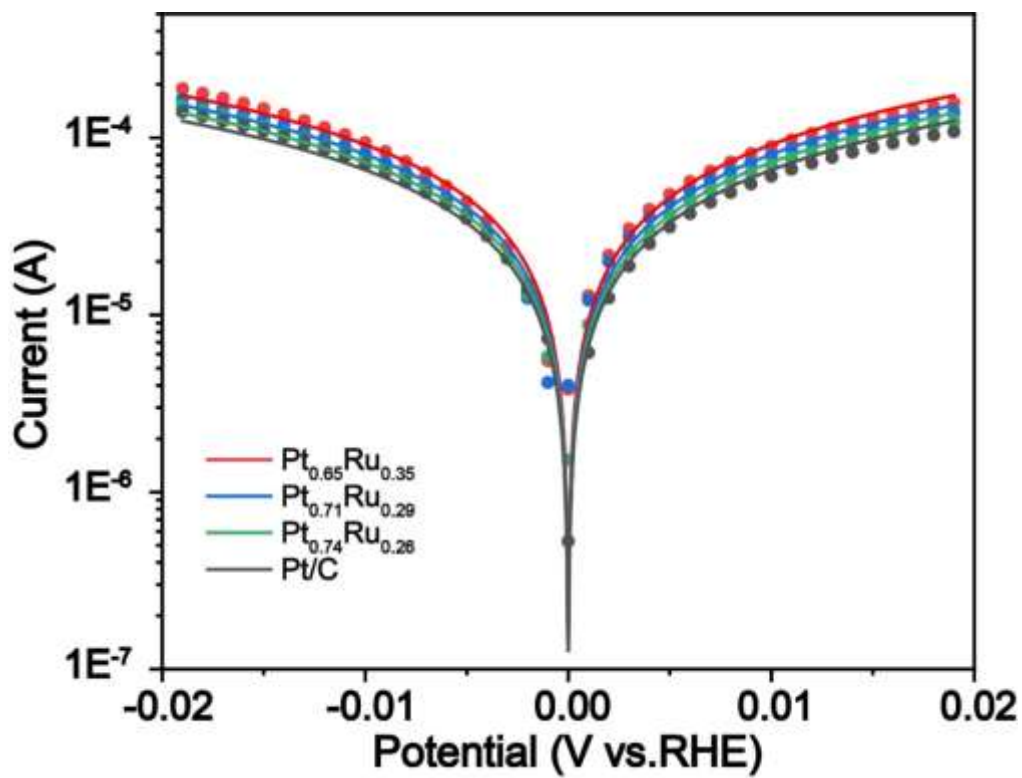


Figure S4. Tafel plots of PtRu bimetallic nanoparticles and Pt/C.

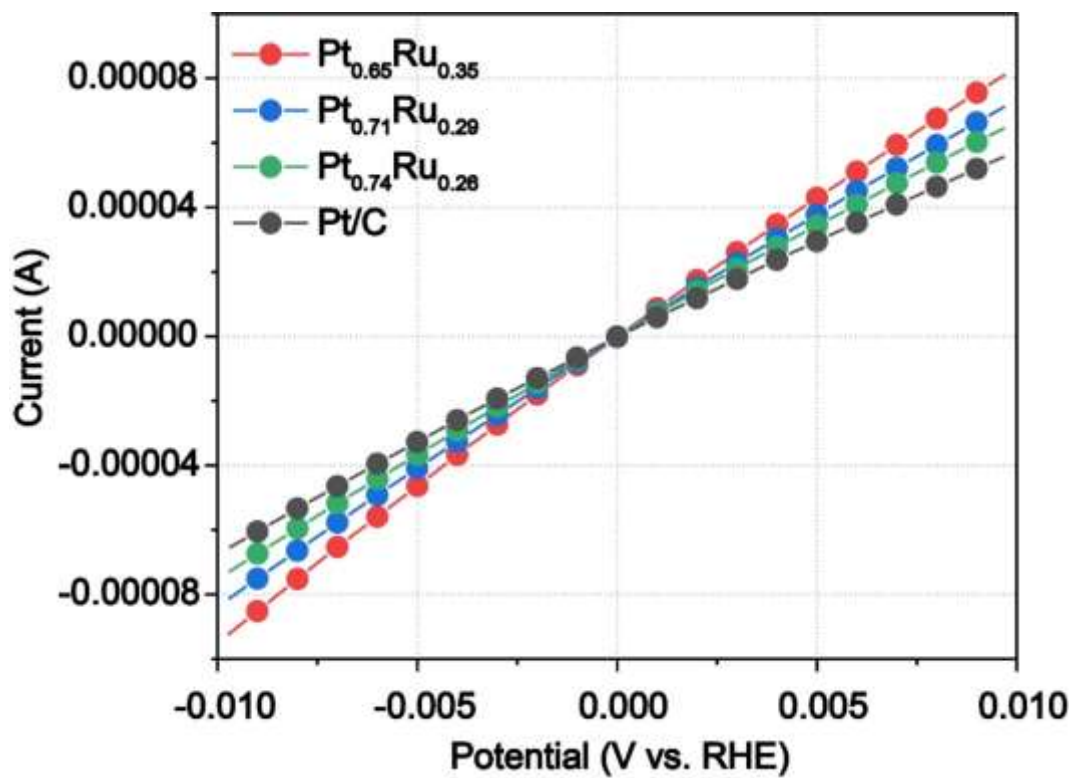


Figure S5. Micro-kinetic polarization plots of PtRu bimetallic nanoparticles and Pt/C.

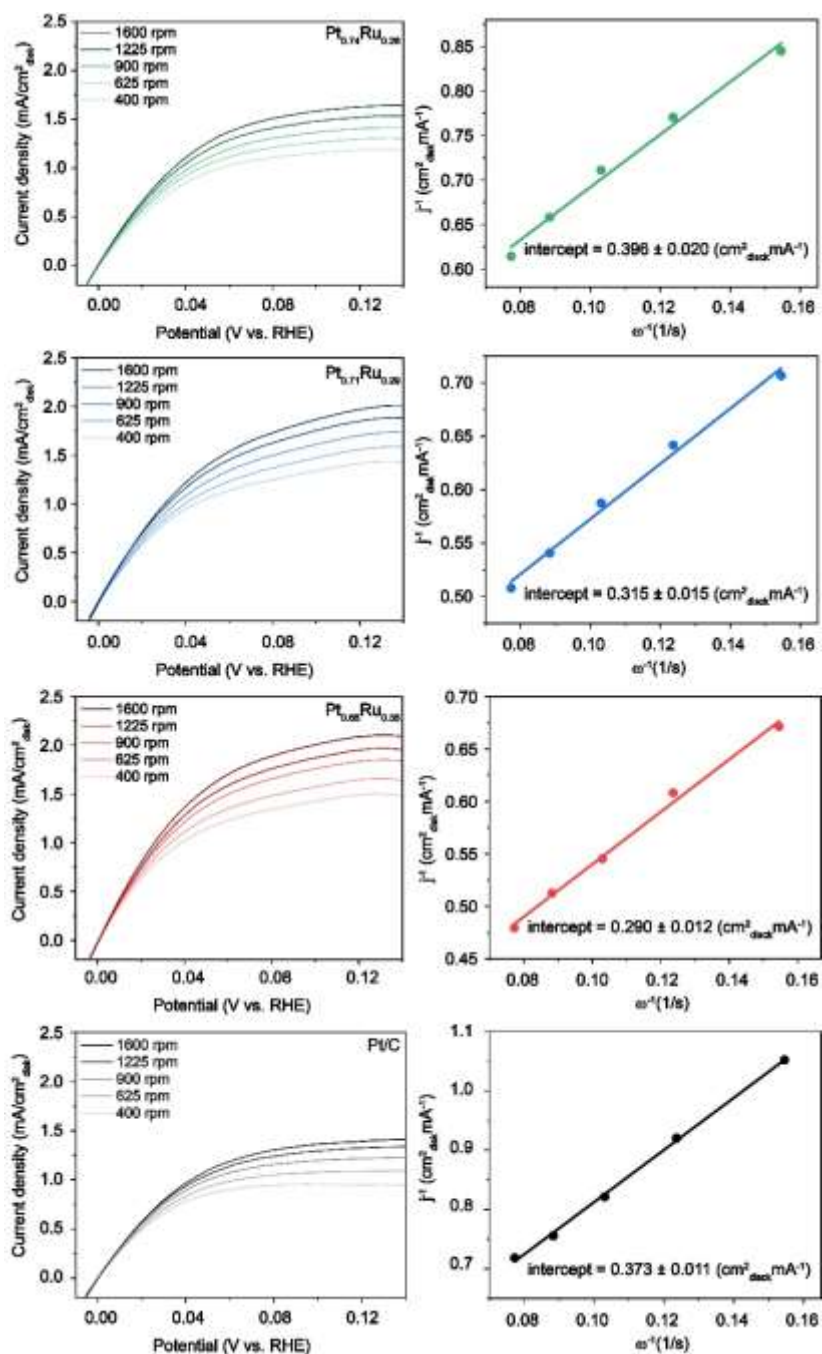


Figure S6. Polarization curves of PtRu bimetallic nanoparticles and Pt/C in H₂-saturated 0.1M KOH at a scan rate of 5mV/s at various rotating speeds. The followed is the corresponding Koutecky–Levich plots at an overpotential of 120mV.

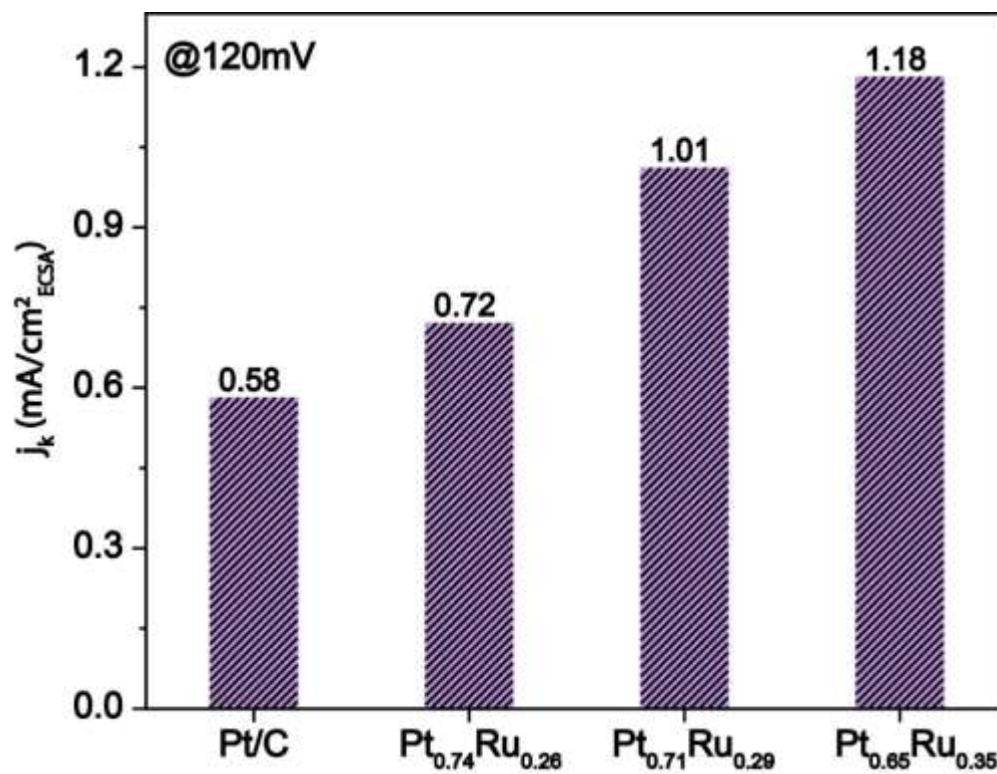


Figure S7. ECSA-normalized kinetic current densities derived from Koutecky–Levich plots for PtRu bimetallic nanoparticles and Pt/C at overpotential of 120 mV.

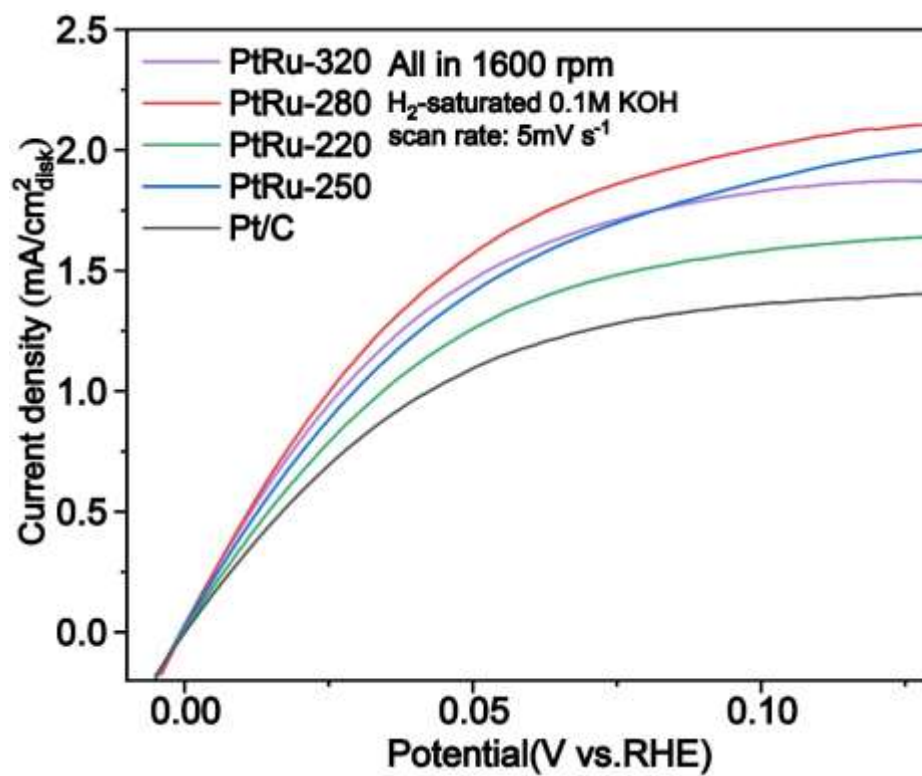


Figure S8. HOR activity comparison. PtRu bimetallic nanoparticles prepared under different temperature.

Table S1. Summary of ICP-MS results for PtRu bimetallic nanoparticles.

| | PtRu-220 | PtRu-250 | PtRu-280 | PtRu-320 |
|-------------------|----------|----------|----------|----------|
| ratio of Pt | 74% | 71% | 65% | 62% |
| ratio of Ru | 26% | 29% | 35% | 38% |
| Lattice parameter | 3.91 | 3.90 | 3.89 | 3.91 |

Table S2. Summary of binding energies for Pt 4f_{7/2} and Pt 4f_{5/2} of PtRu-280, PtRu-250, PtRu-220 and Pt/C from XPS results.

| Catalyst | Binding energy (eV) | | | |
|----------|----------------------|------------------------------------|----------------------|------------------------------------|
| | Pt 4f _{7/2} | Pt ²⁺ 4f _{7/2} | Pt 4f _{5/2} | Pt ²⁺ 4f _{5/2} |
| PtRu-280 | 71.66 | 72.61 | 75.01 | 75.96 |
| PtRu-250 | 71.56 | 72.36 | 74.91 | 75.71 |
| PtRu-220 | 71.41 | 72.26 | 74.76 | 75.61 |
| Pt/C | 71.31 | 72.51 | 74.66 | 75.86 |

Table S3. Summary of electrochemical surface areas for PtRu bimetallic nanoparticles and Pt/C.

| Sample | Electrochemical surface area (m ² /g) |
|----------|--|
| Pt/C | 50.5 |
| PtRu-220 | 34.45 |
| PtRu-250 | 31.42 |
| PtRu-280 | 28.42 |

Table S4. Normalized exchange current densities for PtRu bimetallic nanoparticles and Pt/C.

| Sample | j_0 Micropolarization (mA/cm ² _{ECSA}) | j_0 Butler-Volmer fitting (mA/cm ² _{ECSA}) |
|----------|--|--|
| PtRu-280 | 4.16 | 4.00 |
| PtRu-250 | 3.41 | 3.28 |
| PtRu-220 | 2.75 | 2.64 |
| Pt/C | 1.89 | 1.76 |